

# Enhancement of the crystallization and thermal stability of polyhydroxybutyrate by polymeric additives

Shinn-Gwo Hong · Tsung-Kai Gau ·  
Shih-Che Huang

Received: 15 July 2010 / Accepted: 9 November 2010 / Published online: 8 December 2010  
© Akadémiai Kiadó, Budapest, Hungary 2010

**Abstract** The crystallization and thermal degradation of polyhydroxybutyrate (PHB) blended with a small amount of carboxyl-terminated butadiene acrylonitrile rubber (CTBN) and biocompatible polyvinylpyrrolidone (PVP) are analyzed by differential scanning calorimetry (DSC), dynamic thermogravimetric analysis (TG), gel permeation chromatography (GPC), polarized optical microscope (POM), and wide angle X-ray diffraction (WAXD). From results of DSC, TG, and GPC, it is shown that the presence of PVP or CTBN could affect the crystallization rate, crystallinity, melting temperature, and thermal stability of PHB. The changes of crystal sizes by the added CTBN and PVP are also confirmed by the POM and WAXD analyses. The addition of the 1 wt% PVP or CTBN into PHB can significantly increase the crystallization rate and thermal degradation temperature, and affect the degradation kinetics of PHB due to the steric hindrance effects of the added PVP and CTBN on retarding the degradation reaction. The best improvement of the thermal stability is obtained from the PVP-modified PHB. The method of using CTBN or PVP to improve the thermal stability of PHB is of great processing advantages in industry because it is functional with low purity PHB, henceforth, saves the cost of the purification process.

**Keywords** Polyhydroxybutyrate · Additives · Carboxyl-terminated butadiene acrylonitrile rubber · Polyvinylpyrrolidone · Degradation · Crystallization

## Introduction

The study of biosynthesized polyhydroxyalkanoates (PHAs) attracts growing attention not only because of their special biodegradation and biocompatibility properties, but also due to the increasing concerns of maintaining sustainable environments and alleviating the possible oil shortage problem. Among all different PHAs, the properties of the relatively easier biosynthesized polyhydroxybutyrate (PHB) are mostly studied since its early appearance in the 1920s [1–9]. The impressing biodegradation and biocompatibility properties of PHB have resulted in many potential applications of PHB in the industry especially in the medical field, nonetheless, the inherent brittleness and inferior thermal stability (in addition to cost) have blocked the popular usage of PHB.

The brittleness of PHB is generally resulted from its high crystallinity and post-crystallization behaviors, which result in irregular pores that formed on the surface and limit the flexibility of amorphous chains. To ease this problem, lots of methods such as annealing the molded PHB at a high temperature, cold-drawing of PHB, blending PHB with other thermoplastics (e.g., cellulose, polyethylene, polyesters, poly(vinyl chloride), poly(methyl methacrylate), poly( $\epsilon$ -caprolactone), poly(lactic acid), poly(*cis*-1, 4-isoprene), poly(vinyl acetate), poly(vinyl alcohol), poly(vinylidene fluoride), poly(vinyl alcohol), poly(ethylene oxide), epoxidized natural rubber, etc.), adding low molecular weight plasticizers into PHB, adding organic or inorganic nucleating agents, and copolymerizing PHB with flexible constituents (e.g., 3-hydroxyvalerate (HV) and 3-hydroxyhexanoate (HHx)) are used and lots proven to be effective on improving the toughness of PHB [8–19].

Among mentioned toughening methods, some can also concurrently enhance the thermal stability of PHB, e.g., blending PHB with more stable polymers and adding the

S.-G. Hong (✉) · T.-K. Gau · S.-C. Huang  
Department of Chemical Engineering and Materials Science,  
Yuan-Ze University, Chung-Li 320, Taiwan  
e-mail: cesghong@saturn.yzu.edu.tw

HV and HHx to form PHB copolymers with lower melting temperatures than PHB. The copolymerization broadens the processing window of PHB materials and then the use of a low molding temperature generates less thermal degradation. The additions of compatible thermoplastics and plasticizers have a similar effect on lowering the molding temperature of PHB. Additionally, the thermal stability of PHB can also be improved by chemically attaching various unsaturated chemicals, such as acrylics (methyl methacrylate, 2-hydroxyethyl methacrylate, and acrylic acid), maleic anhydride, and styrene, onto PHB chains through the hindrance of the degradation reaction from the grafted chemicals [11, 14, 20–24].

As indicated, the thermal stability of PHB can be enhanced by adding suitable constituents to lower the melting (or processing) temperature of PHB or block the formation of cyclic rings during the degradation. It is generally accepted that the thermal degradation reaction of PHB is a non-radical random chain scission and *cis*-elimination reaction of  $-\text{CH}$  including a six-membered ring transition [25, 26]. Consequently, the methods shown above are practical routes to ease the thermal degradation of PHB because it usually cannot be effectively inhibited by just adding conventional stabilizers or antioxidants.

In the previous studies, the thermal stability of PHB is shown to be significantly improved by chemical methods, i.e., grafting maleic anhydride and maleic acid onto PHB by various techniques [23, 24]. In this study, it is shown that a simple physical method, i.e., the addition of a small amount of tough carboxyl-terminated butadiene acrylonitrile rubber (CTBN) or biocompatible polyvinylpyrrolidone (PVP) polymeric additives, can also result in different changes and improvements of the crystallization and degradation behaviors of PHB.

## Experimental

### Materials

The as-received PHB is biosynthesized from *E. coli* with crude glucose as the medium (98% pure, hermetically stored in a refrigerator below 0 °C, with the weight-average molecular weight ( $M_w$ ) = 717188 g/mol and polydispersive index (PDI) = 1.55, containing residual  $\text{Ca}^{2+}$  (702 ppm) and  $\text{Mg}^{2+}$  (94 ppm)) and used without further purification. Two polymeric additives, carboxyl-terminated butadiene acrylonitrile rubber (CTBN, with  $M_w$  = 107760, PDI = 3.60) and polyvinylpyrrolidone (PVP, with  $M_w$  = 1.6–2.0 millions g/mol) are obtained from Zeon Chemicals and International Specialty Products, respectively, and used as-received. Different parts of CTBN and PVP are mixed with PHB to form 2 wt% chloroform solutions at 55 °C for 48 h and then cast into films

and dried at the room temperature for 24 h with a thickness about 30  $\mu\text{m}$ . The prepared films are all stored in the refrigerator below  $T_g$  before analysis to avoid further crystallization during storage.

The molecular weights of prepared specimens are measured using gel permeation chromatography (GPC) at 25 °C. GPC is consisted of columns of PLgel 5  $\mu$  10000 A, 5  $\mu$  Guard, and 5  $\mu$  Mixed-C from Polymer Lab., a RI detector L-2490 from Hitachi, and a PU-980 Intelligent HPLC pump from Jasco. Chloroform is used as the eluent at a flow rate of 1 mL/min. The PHB concentration of 20.0 mg/mL is prepared for GPC analysis. The polystyrene standards with different molecular weights (580–841700 g/mol) are used to calibrate GPC results.

### DSC analyses

A Perkin-Elmer DSC-7 is used to measure the DSC heating and cooling curves of different specimens. The DSC curve is measured at a scanning rate of 10 °C/min from  $-40$  to 185 °C (first heating scan), stayed at 185 °C for 5 min to erase the thermal history, subsequently cooled to  $-40$  °C at a cooling rate of 10 °C/min (cooling scan), and then reheated to 185 °C at a scanning rate of 10 °C/min (second heating scan), under the nitrogen environment with a nitrogen flow rate of 40 mL/min. Three specimens prepared from hermetic aluminum (Al) pans are tested for each DSC measurement. The DSC curves obtained are calibrated by the baseline obtained from the empty Al pans and the indium standard.

### Wide angle X-ray diffraction and polarized optical microscope analyses

The wide angle X-ray diffraction (WAX) patterns of specimens after isothermally crystallized at 105 °C for an hour (cooled from 185 °C at a cooling rate of 30 °C/min after 5 min stay at 185 °C) are taken using an XRD-6000 (Shimadzu Co., Japan, Cu ( $K\alpha$ ) at 40 kV and 30 mA) from 2° to 40° at a scanning speed of 1°/min. The optical images of the specimens isothermally crystallized at the same condition are obtained from a Nikon polarized optical microscope (POM) equipped with a Mettler FP90 heating stage.

### TG analyses

The prepared specimens are further analyzed with a Perkin-Elmer Thermogravimetric Analyzer (TG) Pyris-1. The mass-loss behavior of the specimen is measured with a dynamic scanning mode. The specimen is scanned from the room temperature to about 300 °C at the heating rates of 2.5, 5, 10, and 20 °C/min with a nitrogen flow rate of

40 mL/min. The peak temperatures of derivative mass-loss curves, mass-loss percentages, and thermal degradation characteristics are obtained from TG curves.

## Results and discussion

### DSC results

The representative DSC heating curves obtained from the first heating scan of five PHB specimens are shown in Fig. 1 and Table 1 for comparison purposes. As observed in Fig. 1, the PHB and PHB with polymeric additives all have similar melting curves, which have a relative smaller melting peak near 155.4–157.9 °C and a larger melting peak near 168.5–170.2 °C with the melting heat of 83.4–90.5 J/g, because of the similar thermal history, i.e., crystallized from the cast films during solvent evaporation (see Table 1). The multiple melting curves of PHB observed in Fig. 1 are mainly attributed to (1) melting, recrystallization, and remelting during the DSC scanning condition, and (2) crystals with different sizes, lamellar thicknesses, and perfection [11, 23, 24, 27–30]. Henceforth, the low temperature small shoulders in Fig. 1 are resulted from the melting of low temperature melted imperfect crystals formed during the solvent crystallization, while the concave downward region between two endothermic peaks is partly due to the exothermic recrystallization happening after the previous melting process.

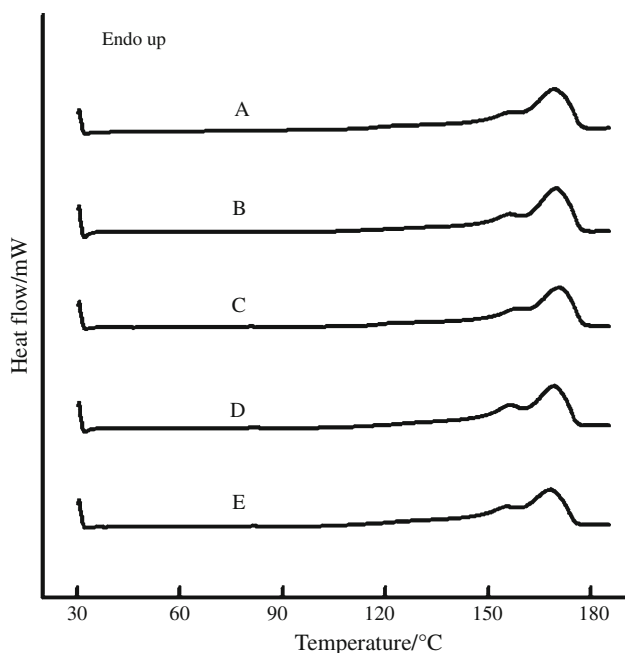


**Fig. 1** The representative DSC 1st heating curves obtained from the (A) PHB, (B) PHB–1CTBN, (C) PHB–2CTBN, (D) PHB–1PVP, and (E) PHB–2PVP

As regards the crystals better formed during the solvent crystallization and melting-recrystallization, they would result in the DSC heating curve with the higher  $T_m$  seen in Fig. 1.

The objective differences in cooling crystallization of various specimens can be obtained by comparing the cooling curves taken after the first heating scan and 5-min isothermal stay at 185 °C from five specimens shown in Fig. 2. As seen in Fig. 2A, the PHB has a small broad exothermic peak starting from 86.4 °C with a peak crystallization temperature ( $T_C$ ) near 71.0 °C which are much greater than those obtained previously from the degraded room temperature stored PHB (see Table 1) [23, 24]. The crystallization temperature of the PHB would start at a higher temperature when CTBN or PVP is added. It is shown in Fig. 2B and C that the PHB blended with 1 and 2 wt% CTBN (referred to as PHB–1CTBN and PHB–2CTBN, respectively) both have narrower crystallization curves beginning at 101.7 and 102.5 °C with  $T_C$  near 88.4 and 90.6 °C, respectively, which are all significant higher than those from the PHB (Table 1). As regards the PHB blended with 1 and 2 wt% PVP (referred to as PHB–1PVP and PHB–2PVP, respectively), two narrow crystallization curves beginning at relatively high 106.4 and 102.2 °C with  $T_C$  near 96.7 and 89.1 °C are also obtained, respectively (see Fig. 2D–E; Table 1). The results indicate that the crystallization rate of the PHB can be noticeably increased by adding a small amount of CTBN or PVP. From the  $T_C$  obtained, the crystallization rates of specimens are in the order of the PHB  $\ll$  PHB–1CTBN  $\sim$  PHB–2PVP  $\sim$  PHB–2CTBN  $<$  PHB–1PVP.

In addition, the crystallization heat ( $\Delta H_c$ ) or crystallinity obtained from the PHB with CTBN and PVP are also higher than that from the PHB. From Table 1, the  $\Delta H_c$  of specimens are in the order of the PHB  $<$  PHB–2PVP  $\sim$  PHB–2CTBN  $<$  PHB–1CTBN  $\sim$  PHB–1PVP. Although the differences among  $\Delta H_c$  are not as great as those among  $T_C$ , it is clear that the addition of CTBN or PVP into PHB would also effectively improve the crystallinity. The best improvement is from the PHB–1PVP.

The relatively smaller crystallinity and slower crystallization rate obtained from the PHB are mainly due to the thermal degradation happening during the DSC test. It is shown in Table 2 that the Mw of the PHB drastically decreases to 82790 (PDI = 1.58) from 717188 g/mol after only 5 min stay at 185 °C. The premature thermal degradation is resulted from residual  $\text{Ca}^{2+}$  and  $\text{Mg}^{2+}$  catalytic impurities in the PHB [23–26, 31–34]. As shown previously, this decrease of Mw or chain lengths would cause a slow crystallization speed and small crystallinity in PHB [23, 24, 35].

The decrease of the molecular weight is also obtained from the CTBN added PHB. As shown in Table 2, the

**Table 1** The average characteristics obtained from DSC curves

DSC scan PHB specimen	1st Heating scan		Cooling scan		2nd Heating scan	
	$T_m/^\circ\text{C}^a$	$\Delta H_m/\text{J/g}^b$	$T_c/^\circ\text{C}^a$	$\Delta H_c/\text{J/g}^b$	$T_m/^\circ\text{C}^a$	$\Delta H_m/\text{J/g}^b$
PHB	169.3 (156.7)	84.9	71.0 (86.4) <sup>c</sup>	59.2	163.8 (150.5)	80.4
PHB-1CTBN	168.5 (155.4)	88.6	88.4 (101.7)	67.5	168.0 (157.3)	88.3
PHB-2CTBN	169.1 (156.0)	83.4	90.6 (102.5)	63.2	165.0 (153.4)	80.2
PHB-1PVP	170.2 (157.1)	85.7	96.7 (106.4)	67.7	163.8 (170.7)	78.8
PHB-2PVP	170.1 (157.9)	90.5	89.1 (102.2)	62.7	169.4 (161.5)	80.6

<sup>a</sup> The larger peak  $T_m$  and (the smaller peak  $T_m$ ). The standard deviations ( $\sigma$ ) are all smaller than 2 °C except the  $T_c$  and  $T_m$  (2nd scan) of the PHB ( $\sigma = 5$  °C)

<sup>b</sup> The standard deviation is smaller than 3 J/g

<sup>c</sup> The onset crystallization temperature

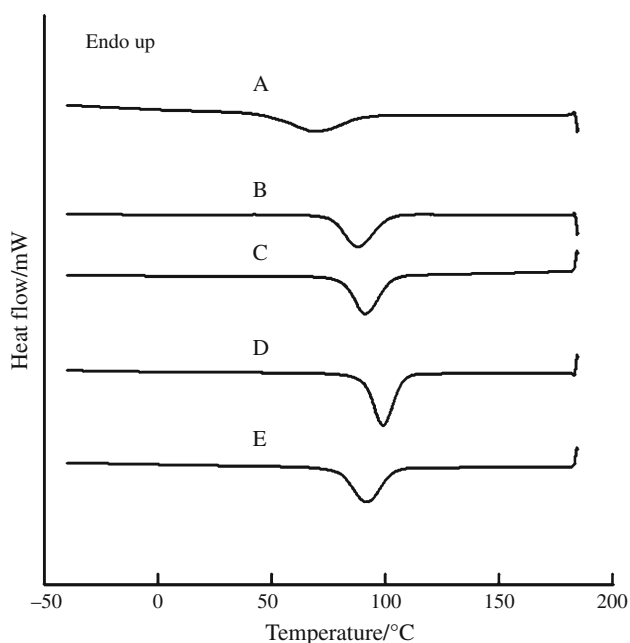


**Fig. 2** The representative DSC cooling curves obtained from the (A) PHB, (B) PHB-1CTBN, (C) PHB-2CTBN, (D) PHB-1PVP, and (E) PHB-2PVP

Mw of PHB-1CTBN and PHB-2CTBN drop to 93600 (PDI = 2.01) and 81870 (PDI = 1.93) g/mol, respectively, after the heating scan. Comparing to those of the PHB, the effect of CTBN on affecting the Mw of PHB changes with the adding amount and which is due to the coincident degradation of CTBN (shown later) with a broad molecular weight distribution (PDI = 3.60). Henceforth, the molecular weight distributions of the PHB-1CTBN and PHB-2CTBN broaden after the DSC thermal stay. Although the addition of CTBN could not effectively stop the decrease of the molecular weight, it promotes the crystallization of PHB due to the presence of flexible chains. It is well known in the industry that the use of crystallization promoters, e.g., the addition of polyethyleneglycol in polyesters, can effectively improve the crystallization of polymers. The

**Table 2** The molecular weights of PHBs after DSC 1st heating scan

PHB specimens	Molecular weight		
	Mn	Mw	PDI
Pristine PHB	52380	82790	1.58
PHB-1CTBN	46530	93600	2.01
PHB-2CTBN	42490	81870	1.93
PHB-1PVP	147580	240150	1.63
PHB-2PVP	152370	245800	1.61

*Mn* number-average molecular weight, *Mw* weight-average molecular weight, *PDI* polydispersive index

flexible CTBN with a very low glass transition temperature can act like a crystallization promoter in PHB and impart additional chain mobility to promote the crystallization.

Different from that of CTBN, it is interesting to note that the decrease of Mw and slow crystallization of PHB can be simultaneously improved by adding a small amount of PVP. It is shown in Table 2 that the PHB-1PVP and PHB-2PVP have Mw near 240150 (PDI = 1.63) and 245800 g/mol (PDI = 1.61) after the high temperature stay, respectively. These Mw are obviously much greater than those of other specimens. Although the Mw of PVP is near 1.6–2.0 millions, the addition of 1 or 2 wt% into PHB would not result in such a great Mw after the degradation. As a result, the observed large Mw is from the improvement of the thermal stability of the PHB and which is resulted from the possible inhibition of six-member cyclic ring formation by the steric hindrance offered by the added long chain PVP molecules. This is confirmed by TG results shown later. Therefore, the less degraded PHB-1PVP and PHB-2PVP have the higher crystallization rates and crystallinity. This result is consistent with those obtained from the grafted PHB [23, 24].

The extents of crystallization of tested specimens can also be compared using the second heating DSC curves shown in Fig. 3. Similar to that in Fig. 1A, the PHB has two melting peaks, a smaller peak with a lower  $T_m$  near 150.5 °C and a larger peak with a higher  $T_m$  near 163.8 °C,

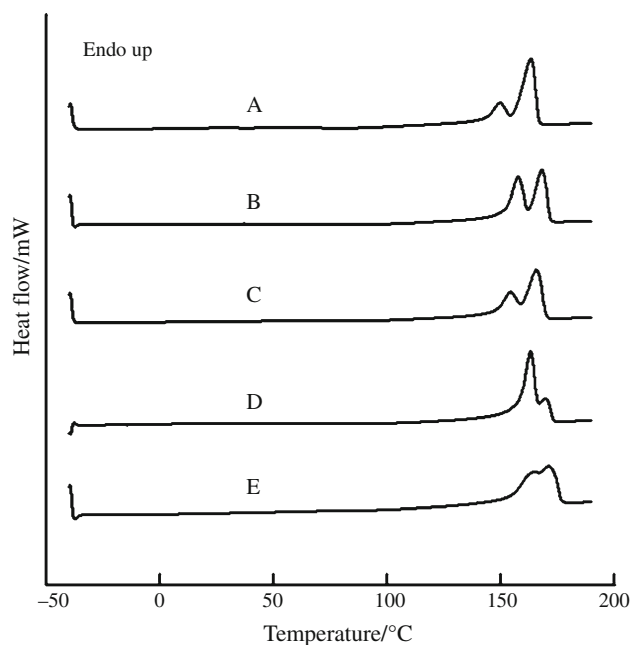


**Fig. 3** The representative DSC 2nd heating curves obtained from the (A) PHB, (B) PHB-1CTBN, (C) PHB-2CTBN, (D) PHB-1PVP, and (E) PHB-2PVP

after the cooling crystallization (Table 1). Both the two melting temperatures are lower than those in Fig. 1A because the significant decrease of Mw after the first heating scan results in the formation of inferior crystals. This also results in the much larger melting peak at the higher  $T_m$  and a larger  $\Delta H_m$  than  $\Delta H_c$  obtained due to the significant melting-recrystallization and secondary crystallization (Table 1).

As regards the PHB with CTBN, different second DSC heating curves are obtained. It is shown in Fig. 3B and C that the PHB-1CTBN and PHB-2CTBN have two separate melting peaks but with  $T_m$  all greater than those from the PHB and with less larger peaks at the higher  $T_m$  (see Table 1). As obtained previously from Fig. 2, the PHB-1CTBN and PHB-2CTBN have faster crystallization rates and larger crystallinity than the PHB, henceforth, would have better crystals formed. This better crystallization results in the higher  $T_m$  and also the relatively larger melting peaks at the lower  $T_m$  because of the less melting-recrystallization. It is reasonable that the PHB-1CTBN has the higher  $T_m$  and larger low  $T_m$  peak than the PHB-2CTBN due to a higher  $\Delta H_c$  obtained.

The changes in melting peaks can be more clearly observed from the PVP added PHB. As seen in Fig. 3D and E, the PHB-1PVP and PHB-2PVP (with the greatest Mw than other specimens) have the higher  $T_m$  than other specimens because of the better crystals formed from less degraded specimens. (see Table 1). It is obvious that the

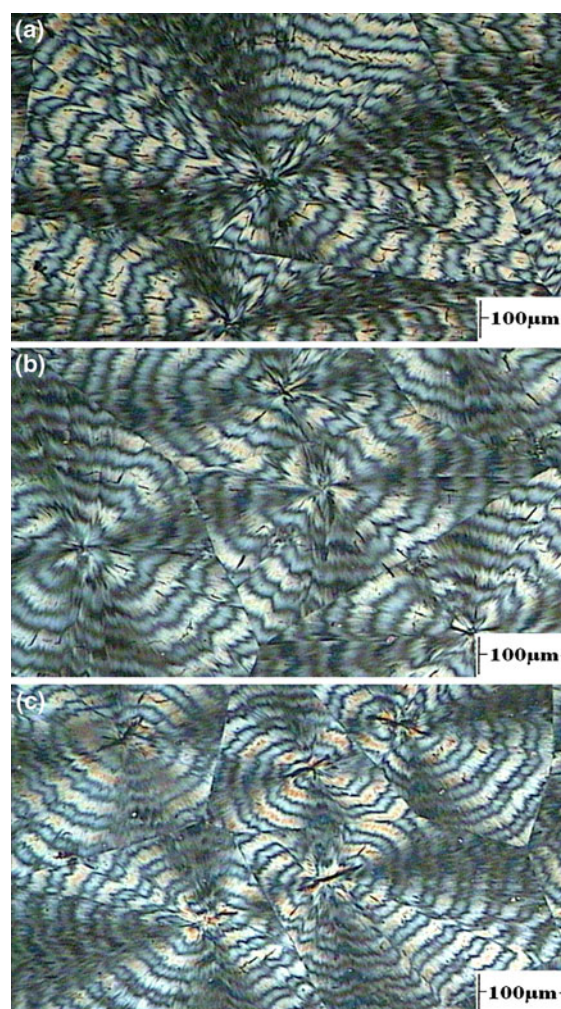


**Fig. 4** The representative POM images obtained from the a PHB, b PHB-1CTBN, and c PHB-1PVP after isothermally crystallized at 105 °C

PHB-1PVP has the best crystallization and the greatest  $T_m$  among all specimens because it has the highest  $T_c$ ,  $\Delta H_c$ , and melting peak at the lower  $T_m$  (the least melting-recrystallization).

In addition, the presence of PVP or CTBN can also change the crystal size of PHB. It is shown in Fig. 4 that the PHB, PHB-1CTBN, and PHB-1PVP all exhibit typical spherulites with clear Maltese cross patterns but different spherulite sizes. The spherulite sizes of the PHB are in the range of 350–500  $\mu\text{m}$  which are obviously greater than the range of 250–350  $\mu\text{m}$  from the PHB-1CTBN and PHB-1PVP. This result is consistent with the DSC cooling results. The PVP and CTBN could act as nucleating agents and result in the formation of smaller spherulites.

The WAXD patterns of the representative specimens are also shown in Fig. 5 and from which the effects of

added modifiers on PHB crystal structures can be obtained. As seen, the basic WAXD patterns from the  $\alpha$ -form crystals of PHB are observed in all specimens but with differences in relative intensities of diffraction peaks mostly due to lamellae orientation differences in limited film specimens with different spherulite sizes [36]. It is clear in Table 3 that the lattice parameters from the PHB, PHB-1CTBN, and PHB-1PVP have few differences and are similar to those published elsewhere. However, the mean sizes of the ordered domains (the shape factor) related to different crystallographic planes calculated using the Scherrer equation indicate that the addition of few PVP can significantly change the ordered domain sizes while the effect of CTBN on the calculated values is not obvious by comparing with those of the PHB (see Table 3).

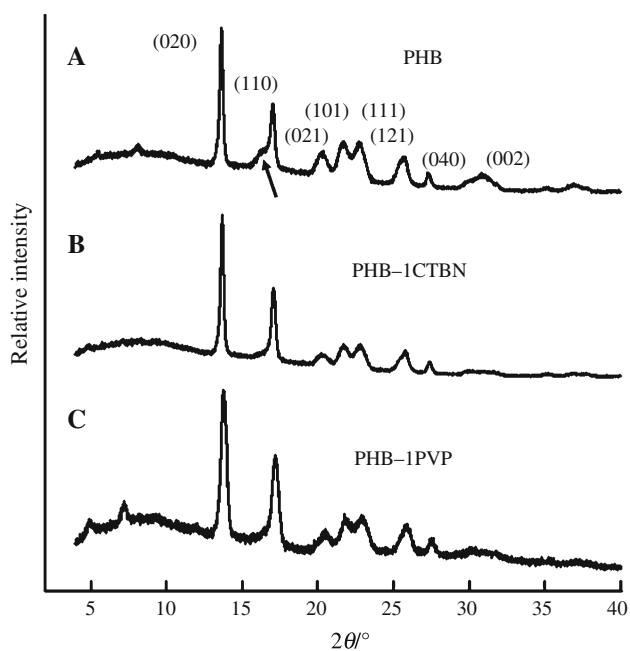


**Fig. 5** The representative WAXD patterns obtained from the (A) PHB, (B) PHB-1CTBN, and (C) PHB-1PVP after isothermally crystallized at 105 °C

**Table 3** The estimated mean sizes of ordered domains ( $D$ ) and lattice parameters ( $a$ ,  $b$ , and  $c$ ) of specimens after isothermally crystallized at 105 °C from WAXD analyses

Sample	$D$ (020)/ nm	$D$ (110)/ nm	$D$ (040)/ nm	$a/\text{Å}$	$b/\text{Å}$	$c/\text{Å}$
PHB	33.3	24.3	23.4	5.73	13.08	5.82
PHB-1CTBN	34.8	26.8	23.4	5.64	13.02	5.92
PHB-1PVP	17.8	16.4	17.8	5.64	12.93	5.87

## TG results

The effects of PVP and CTBN on the thermal degradation of PHB are obtained from TG analyses. From Fig. 6, the representative TG curves taken from five specimens at a scanning rate of 10 °C/min, it is obvious that the onset temperatures ( $T_o$ ) and the peak temperatures ( $T_p$ ; the temperature at the maximal mass loss rate) of different specimens follow the order of the PHB < PHB-2CTBN < PHB-1CTBN ~ PHB-2PVP < PHB-1PVP (see Fig. 7; Table 4). As a result, the PHB specimens blended with CTBN and PVP all have significantly higher  $T_o$ ,  $T_p$ , and better thermal stability than the PHB. The PHB-1PVP clearly has the best thermal stability.

It is important to note that the noticeable improvement of thermal stability can also be obtained from the purified PHB with catalytic  $\text{Ca}^{2+}$  and  $\text{Mg}^{2+}$  impurities removed. This confirms that the enhancing effects of PVP and CTBN are not from their reactions with the impurities but from their steric hindrance effects on retarding the formation of six-member cyclic rings. Consequently, the method of using CTBN and PVP to improve the thermal stability of PHB is of great processing advantages in industry because

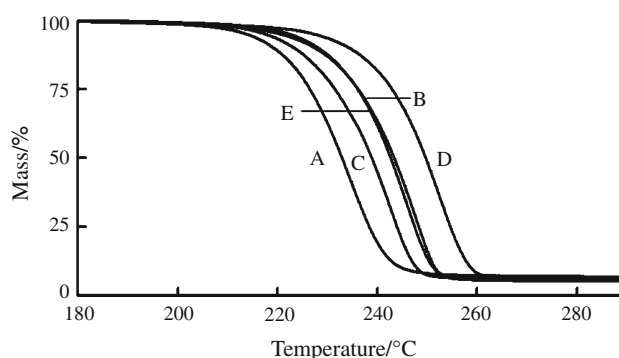


**Fig. 6** The representative TG curves obtained from the (A) PHB, (B) PHB-1CTBN, (C) PHB-2CTBN, (D) PHB-1PVP, and (E) PHB-2PVP at a heating rate of 10 °C/min

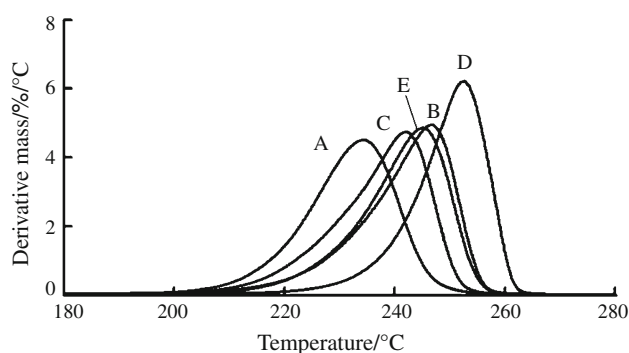


**Fig. 7** The representative DTG curves obtained from the (A) PHB, (B) PHB-1CTBN, (C) PHB-2CTBN, (D) PHB-1PVP, and (E) PHB-2PVP at a heating rate of 10 °C/min

**Table 4** The representative degradation temperatures obtained from TG curves of PHBs at a scanning rate of 10 °C/min

PHB specimens	PHB	PHB-1CTBN	PHB-2CTBN	PHB-1PVP	PHB-2PVP
$T_d/^\circ\text{C}^*$	185.4	201.1	196.7	202.5	199.2
$T_p/^\circ\text{C}^*$	234.6	246.5	242.1	252.2	246.5

\* The standard deviation is smaller than 3 °C

it is effective in less purified PHB, henceforth, decreases the cost of the purification process.

The thermal degradation of CTBN and PVP additives are also analyzed by TG. In general, the CTBN has a minor mass loss peak near 220 °C with a  $T_o$  about 150 °C and 3% mass loss mostly due to low molecular weight products formed during the synthesis. The main degradation of the CTBN starts about 330 °C with a  $T_p$  near 469 °C and a major mass loss about 93%. The early small degradation of the CTBN is related to the decreases of the Mw of the PHB-1CTBN and PHB-2CTBN shown in Table 2 but obviously it does not adversely affect the thermal stability of PHB. It is believed that the more thermal stable main portions of the CTBN offer PHB steric hindrance and then improve its thermal stability.

Regarding the PVP used, the TG result indicates that it starts the mass loss near 350 °C with a  $T_p$  about 448 °C and loses almost all its mass with an end temperature near 490 °C. The addition of the stable PVP not only causes the greatest retention of Mw of the PHB-1PVP and PHB-2PVP shown in Table 2 but also adds barriers to block the degradation reaction and results in the significant improvement of the thermal stability (see Table 4).

From the representative DTG curves shown in Fig. 7, it is clear that the PHB has a relatively less asymmetric DTG curve, while other four PHB specimens all have more asymmetric curves with small long tails (i.e., small mass loss rates) on the low temperature side. The ratio of mass loss rates on the left-hand and right-hand side of the peak in the DTG curve, the so-called symmetric index, has been proposed by Kissinger and used by many investigators to compare the different kinetic factors obtained from the degradation reaction [37]. As a result, the clear difference in shapes of DTG curves between the PHB and the blended PHB specimens qualitatively indicates that the PVP and CTBN added can change the degradation kinetic characteristics of PHB. This is consistent with those obtained previously from changes of  $T_p$  in different specimens and is confirmed below by the different activation energies obtained.

The degradation of specimens is further analyzed using the dynamic scanning method (see representative TG curves in Fig. 8). The activation energies of the degradation reaction at different conversions are calculated using the isoconversion plots proposed in the Flynn–Wall–Ozawa method [38, 39]. As observed in Fig. 9 and Table 5,

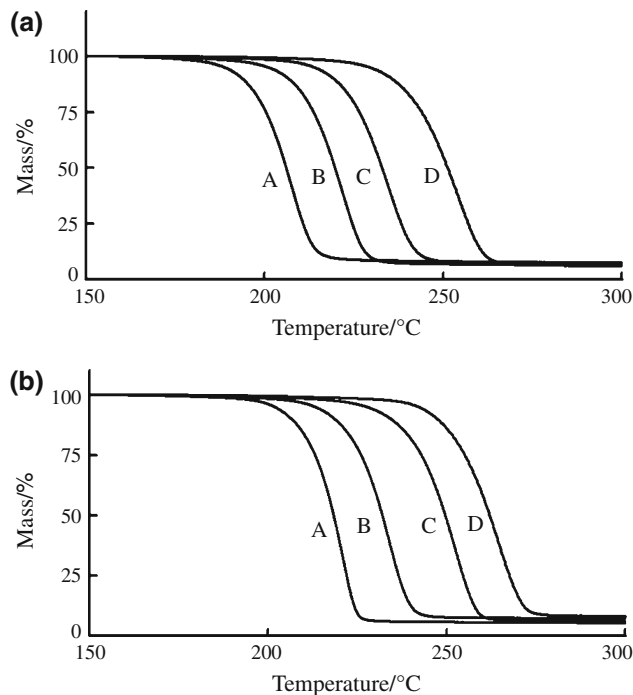


**Fig. 8** The representative dynamic TG curves obtained from the **a** PHB and **b** PHB-1PVP at heating rates of (A) 2.5 °C/min, (B) 5 °C/min, (C) 10 °C/min, and (D) 20 °C/min

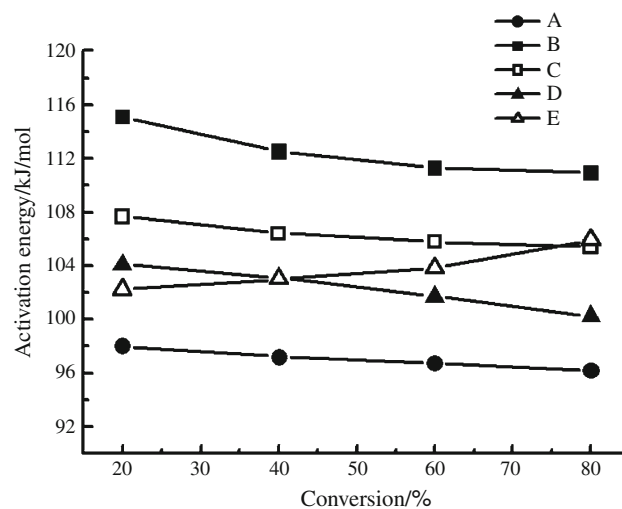


**Fig. 9** The activation energies calculated from isoconversion curves obtained from the dynamic TG curves of the (A) PHB, (B) PHB-1CTBN, (C) PHB-2CTBN, (D) PHB-1PVP, and (E) PHB-2PVP at different conversions

**Table 5** Thermal degradation characteristics calculated from TG curves

Specimens	Activation energy/kJ/mol at different conversions, $\alpha$				
	0.2	0.4	0.6	0.8	Average
PHB	98.0	97.2	96.7	96.2	97.0 (0.7) <sup>a</sup>
PHB-1CTBN	115.1	112.5	111.3	110.9	112.4 (1.8)
PHB-2CTBN	107.7	106.4	105.8	105.4	106.3 (1.0)
PHB-1PVP	104.1	103.1	101.7	100.2	102.2 (1.7)
PHB-2PVP	102.2	103.0	103.8	105.9	103.7 (1.6)

<sup>a</sup> Standard deviation

each of the five specimens has few changes of activation energies (with standard deviations obtained) during the degradation process. This result implies that the thermal degradation reaction of the PHB or PHB blended with CTBN and PVP has a simple mechanism and mainly follows a simple step reaction [23, 24]. However, the average activation energies of the four CTBN and PVP added specimens are all statistically greater than that of the PHB and follow the order of the PHB < PHB-1PVP ~ PHB-2PVP < PHB-2CTBN < PHB-1CTBN. As a result, it is confirmed that the added CTBN and PVP can change the temperature sensitivity or kinetics of the six-member ring formation in the PHB degradation reaction.

## Conclusions

The crystallization and thermal degradation properties of polyhydroxybutyrate (PHB) blended with a small amount of carboxyl-terminated butadiene acrylonitrile rubber (CTBN) and biocompatible polyvinylpyrrolidone (PVP) are obtained. The results indicate that the crystallization rate, crystallinity, crystal size, melting behavior, thermal stability, and degradation kinetics of the PVP and CTBN blended PHB are significantly affected because of the effect of the added PVP and CTBN on retarding the degradation reaction. Both the PVP and CTBN can significantly improve the thermal stability, increase the crystallization rate, and change the degradation kinetics of the PHB. The addition of 1 wt% PVP results in the greatest improvement of the crystallization and degradation behaviors.

## References

- Mas-Castella J, Urmeneta J, Lafuente R, Navarrete A, Guerrero R. Biodegradation of Poly- $[\beta]$ -hydroxyalkanoates in anaerobic sediments. *Int Biodeterior Biodegrad*. 1995;35:155–74.
- Doi Y, Kasuya K, Abe H, Koyama N, Ishiwatari S, Takagi K, Yoshida Y. Evaluation of biodegradabilities of biosynthetic and chemosynthetic polyesters in river water. *Polym Degrad Stab*. 1996;51:281–6.
- Yoon JS, Jung HW, Kim MN, Park ES. Diffusion coefficient and equilibrium solubility of water molecules in biodegradable polymers. *J Appl Polym Sci*. 2000;77:1716–22.
- Iwata T, Shiromo M, Doi Y. Surface structures of poly[(R)-3-hydroxybutyrate] and its copolymer single crystals before and after enzymatic degradation with an extracellular PHB depolymerase. *Macro Chem Phys*. 2002;203:1309–16.
- Doi Y, Mukai K, Kasuya K, Yamada K. Biodegradation of bio-synthetic and chemosynthetic polyhydroxyalkanoates. In: Doi Y, Fukuda K, editors. *Biodegradable plastics and polymers*. Amsterdam: Elsevier; 1994. p. 39–51.
- Kumagai Y, Kanesawa Y, Doi Y. Enzymatic degradation of microbial poly(3-hydroxybutyrate) films. *Makromol Chem*. 1992; 193:53–7.
- Tomasi G, Scandola M, Briese BH, Jendrosseck D. Enzymatic degradation of bacterial poly(3-hydroxybutyrate) by a depolymerase from *Pseudomonas lemoignei*. *Macromolecules*. 1996;29: 507–13.
- Koyama N, Doi Y. Effects of solid-state structures on the enzymatic degradability of bacterial poly(hydroxyalkanoic acids). *Macromolecules*. 1997;30:826–32.
- Zhao K, Deng Y, Chen GQ. Effects of surface morphology on the biocompatibility of polyhydroxyalkanoates. *Biochem Eng J*. 2003; 16:115–23.
- Zheng Z, Bei FF, Tian HL, Chen GQ. Effects of crystallization of polyhydroxyalkanoate blend on surface physicochemical properties and interactions with rabbit articular cartilage chondrocytes. *Biomaterials*. 2005;26:3537–48.
- Chen C, Fei B, Peng S, Zhuang Y, Dong L, Feng Z. Nonisothermal crystallization and melting behavior of poly(3-hydroxybutyrate) and maleated poly(3-hydroxybutyrate). *Eur Polym J*. 2002;38:1663–70.
- Wang L, Zhu W, Wang X, Chen X, Chen GQ, Xu K. Processability modifications of poly(3-hydroxybutyrate) by plasticizing, blending, and stabilizing. *J Appl Polym Sci*. 2008;107:166–73.
- Zhao Q, Cheng G, Song C, Zeng Y, Tao J, Zhang L. Crystallization behavior and biodegradation of poly(3-hydroxybutyrate) and poly(ethylene glycol) multiblock copolymers. *Polym Degrad Stab*. 2006;91:1240–6.
- Lee HK, Ismail J, Kammer HW, Bakar MA. Melt reaction in blends of poly(3-hydroxybutyrate) (PHB) and epoxidized natural rubber (ENR-50). *J Appl Polym Sci*. 2005;95:113–29.
- Kaito A. Unique orientation textures formed in miscible blends of poly(vinylidene fluoride) and poly[(R)-3-hydroxybutyrate]. *Polymer*. 2006;47:3548–56.
- El-Taweel SH, Stoll B, Hohne GWH, Mansour AA, Seliger H. Stress-strain behavior of blends of bacterial polyhydroxybutyrate. *J Appl Polym Sci*. 2004;94:2528–37.
- Stefani PM, Ruseckaite RA, Vázquez A. Poly(3-hydroxybutyrate-co-11 mass% 3-hydroxyvalerate) molded part during the solidification step. *J Therm Anal Calorim*. 2009;95:305–12.
- Malinova L, Brozek J. Mixtures poly((R)-3-hydroxybutyrate) and poly(L-lactic acid) subjected to DSC. *J. Therm. Anal. Calorim*. 2010; Published online: 28 October 2010.
- Rodrigues JAFR, Parra DF, Lugao AB. Crystallization on Films of PHB/PEG Blends. *J Therm Anal Calorim*. 2005;79:379–81.
- Bahari K, Mitomo H, Enjoji T, Yoshii F. Degradability of poly(3-hydroxybutyrate) and its copolymer grafted with styrene by radiation. *Polym Degrad Stab*. 1998;61:245–52.
- Chen C, Peng S, Fei B, Zhuang Y, Dong L, Feng Z, Chen S, Xia H. Synthesis and characterization of maleated poly(3-hydroxybutyrate). *J Appl Polym Sci*. 2003;88:659–68.
- Chen C, Fei B, Peng S, Zhuang Y, Dong L, Feng Z. The kinetics of the thermal decomposition of poly(3-hydroxybutyrate) and



- maleated poly(3-hydroxybutyrate). *J Appl Polym Sci.* 2002;84:1789–96.
23. Hong SG, Lin YC. Improvement of the thermal stability of polyhydroxybutyrates by grafting with maleic anhydride by different methods: differential scanning calorimetry, thermogravimetric analysis, and gel permeation chromatography. *J Appl Polym Sci.* 2008;110:2718–26.
  24. Hong SG, Lin YC. Crystallization and degradation behaviors of treated polyhydroxybutyrates. *React Funct Polym.* 2008;68:1516–23.
  25. Grassie N, Marray EJ, Holmes PA. The thermal degradation of poly(-D)- $\beta$ -hydroxybutyric acid): part 1—identification and quantitative analysis of products. *Polym Degrad Stab.* 1984;6:47–61.
  26. Grassie N, Marray EJ, Holmes PA. The thermal degradation of poly(-D)- $\beta$ -hydroxybutyric acid): part 2—changes in molecular weight. *Polym Degrad Stab.* 1984;6:95–103.
  27. Lee WK, Iwata T, Abe H, Doi Y. Studies on the enzymatic degradation of solution-grown lamellar crystals of poly[(r)-3-hydroxybutyrate]: defects in crystals. *Macromolecules.* 2000;33:9535–41.
  28. Gunaratne LWMK, Shanks RA, Amarasinghe G. Thermal history effects on crystallization and melting of poly(3-hydroxybutyrate). *Thermochim Acta.* 2004;423:127–35.
  29. Gunaratne LWMK, Shanks RA. Melting and thermal history of poly(hydroxybutyrate-co-hydroxyvalerate) using step-scan DSC. *Thermochim Acta.* 2005;430:183–90.
  30. Liu T, Petermann J. Multiple melting behavior in isothermally cold-crystallized isotactic polystyrene. *Polymer.* 2001;42:6453–61.
  31. Kopinke ED, Mackenzie K. Mechanistic aspects of the thermal degradation of poly(lactic acid) and poly([ $\beta$ ]-hydroxybutyric acid). *J Anal Appl Pyrol.* 1997;40–41:43–53.
  32. Kopinke FD, Remmler M, Mackenzie K. Thermal decomposition of biodegradable polyesters—I: poly([ $\beta$ ]-hydroxybutyric acid). *Polym Degrad Stab.* 1996;52:25–38.
  33. Valappil SP, Boccaccini AR, Bucke C, Roy I. Polyhydroxyalkanoates in Gram-positive bacteria: insights from the genera *Bacillus* and *Streptomyces*. *Antonie Van Leeuwenhoek.* 2007;91:1–17.
  34. Kim KJ, Doi Y, Abe HA. Effects of residual metal compounds and chain-end structure on thermal degradation of poly(3-hydroxybutyric acid). *Polym Degrad Stab.* 2006;91:769–77.
  35. Ahmed EH, Rainer S, Ekkehard S, Gert M, Riemschneider M. Effect of melt processing on crystallization behavior and rheology of poly(3-hydroxybutyrate) (phb) and its blends. *Macromol Mater Eng.* 2002;287:363–72.
  36. Canetti M, Urso M, Sadocco P. Influence of the morphology and of the supermolecular structure on the enzymatic degradation of bacterial poly(3-hydroxybutyrate). *Polymer.* 1999;40:2587–94.
  37. Tang W, Li XG, Yan D. Thermal decomposition kinetics of thermotropic copolyesters made from trans-p-hydroxycinnamic acid and p-hydroxybenzoic acid. *J Appl Polym Sci.* 2004;91:445–54.
  38. Flynn JH, Wall LA. General treatment of the thermogravimetry of polymers. *J Res Natl Bur Stand.* 1966;70A:487–523.
  39. Ozawa T. A new method of analyzing thermogravimetric data. *Bull Chem Soc Jpn.* 1965;38:1881–6.